Biosensors and Bioelectronics 161 (2020) 112256

Contents lists available at ScienceDirect

Biosensors and Bioelectronics

journal homepage: http://www.elsevier.com/locate/bios

Dual-output toehold-mediated strand displacement amplification for sensitive homogeneous electrochemical detection of specie-specific DNA sequences for species identification

Ying Zhang [a,b], Wenjun Wang [a], Zhenyu Lin [c,*], Bang Liu [a,**], Xiang Zhou [a,***]

[a] Key Laboratory of Agricultural Animal Genetics, Breeding, and Reproduction of Ministry of Education, College of Animal Science and Technology, Huazhong Agricultural University, Wuhan, 430070, Hubei, PR China

[b] Central Laboratory, Fujian Provincial Key Laboratory of Precision Medicine for Cancer, The First Affiliated Hospital of Fujian Medical University, Fuzhou, Fujian, 350005, China

[c] Ministry of Education Key Laboratory for Analytical Science of Food Safety and Biology, Fujian Provincial Key Laboratory of Analysis and Detection for Food Safety, College of Chemistry, Fuzhou University, Fuzhou, Fujian, 350116, China

ARTICLE INFO

Keywords:
Electrochemical biosensor
Identification of animal species
Signal amplification
Homogeneous detection

ABSTRACT

The determination of specie-specific DNA sequences is a key factor for identification of animal species and detection of meat adulteration. Herein, a simple homogeneous electrochemical biosensor was developed for sensitive detection of specie-specific DNA sequences from meat products based on high efficient and specific dual-output toehold-mediated strand displacement (TMSD). After incubation with target DNA, large amount of methylene blue (electrochemical signal molecule) labeled probes (MB-P) were released from preformed DNA duplex structures by the process of dual-output TMSD amplification. The free MB-P could be further digested by Exonuclease I, and the enzymatic products contain little negative charge could diffuse to the surface of indium tin oxide electrode, generating significantly electrochemical signal. As a result, the designed biosensor showed a broad dynamic range from 0.01 pM to 100 pM, with a low detection limit of 8.2 fM, and ideal selectivity and reproducibility. Meanwhile, the approach exhibited acceptable accuracy for the detection of specie-specific DNA sequences, and possessed the potential application for the identification of animal species from meat products.

1. Introduction

Adulteration of meat and meat products occurs frequently and become a serious social problem worldwide (Hsieh and Ofori, 2014; King et al., 2017; O'Mahony, 2013). Incorporating meat products with cheaper substances or mislabeling meat products on purpose would affect economic interests, cause problems for religious reason and harm the health for many consumers (Ali et al., 2018; Bilge et al., 2016; Doosti et al., 2014). Therefore, species identification plays a critical role in determination of actual species in meat products and fighting against adulteration. Routinely used methods for identification of animal fractions in meat products are DNA (Druml et al., 2015; Lin and Hwang, 2007; Wang et al., 2019) and proteins (Cai et al., 2013; Leitner et al., 2006; Shi et al., 2019) based techniques. Among them, DNA-based polymerase chain reaction (PCR) assays including PCR (Wang et al., 2019), real-time PCR (Druml et al., 2015), PCR restriction fragment length polymorphism (PCR-RFLP) (Lin and Hwang, 2007) and other related assays are common and convenient methods for qualitative and quantitative detection of animal fractions in meat products. However, the successful PCR reaction is significantly depended on DNA quality. Preparation of high-quality DNA from meat products, especially processed meat products has become major concern in PCR-based methods (Piskata et al., 2017). Indeed, the manufacturing process for meat products can degrade DNA to small molecular (Piskata et al., 2019). Fragment size of DNA is a critical limiting factor for PCR reaction, which can significantly affect efficiency of the DNA application and accuracy of animal species determination (Piskata et al., 2017). Therefore, developing an accurate, sensitive and efficient method suitable for small fragment of DNA will enhance testing ability for meat adulteration.

Different techniques, such as fluorescence, colorimetric, and

* Corresponding author. 2 Xue Yuan Road, University Town Fuzhou, Fujian, PR China.
** Corresponding author. No.1 Shizishan Street, Wuhan, Hubei, PR China.
*** Corresponding author. No.1 Shizishan Street, Wuhan, Hubei, PR China.
E-mail addresses: zylin@fzu.edu.cn (Z. Lin), liubang@mail.hzau.edu.cn (B. Liu), zhouxiang@mail.hzau.edu.cn (X. Zhou).

https://doi.org/10.1016/j.bios.2020.112256
Received 24 January 2020; Received in revised form 24 April 2020; Accepted 27 April 2020
Available online 30 April 2020
0956-5663/© 2020 Elsevier B.V. All rights reserved.

electrochemical detection, and so on, were applied to develop biosensors for DNA sequence detection (Chen et al., 2019; Li et al., 2011b; Sapkota et al., 2019; Yang et al., 2017). The electrochemical detection exhibits its inherent advantages of rapid detection, high sensitivity, low cost, and portable devices (Henihan et al., 2016; Koo et al., 2018). Mostly DNA based biosensors need the immobilization of probe DNA on the electrode surface firstly, and target DNA interacts with the probe DNA on the electrode/solution interface. The binding and recognition efficiencies are low because of the electrode surface's spatial hindrance effect. The development of homogeneous electrochemical biosensors based on the difference diffusion ability of long and short DNA to the negative charged indium tin oxide (ITO) electrode surface can overcome this problem easily (Luo et al., 2008). This technique has been applied to detect different analytes, such as small molecular, nucleic acid, protein, etc. (Chang et al., 2019b; Lin et al., 2018; Lu et al., 2017; Wei et al., 2014) But to the best of our knowledge, little attention has been paid to develop homogeneous electrochemical biosensor to distinguish specie-specific genomic DNA sequences and determinate animal species from meat products. Due to the low abundance of target DNA (Li et al., 2011a;Wang et al., 2011), the signal amplification strategy is usually required to obtain sensitive detection. For example, Tan et al. developed an immobilization-free electrochemical biosensor for DNA species related to oral cancer based on nicking endonuclease assisted target recycling amplification. This DNA biosensor can detect as low as 0.35 pM target DNA (Tan et al., 2015). Li et al. reported an electroactive dyes-mediated truly ratiometric homogeneous electrochemical strategy for sensitive miRNA detection, which combined with two ingeniously cascaded signal amplification strategies by Exo III-assisted signal transduction/amplification reaction and hybridization chain reaction (Chang et al., 2019a). The introduction of signal amplification techniques can obviously improve the sensitivity of detection method. Toehold-mediated strand displacement (TMSD) is a powerful enzyme free isothermal strand displacement amplification strategy in DNA nanotechnology (Hong et al., 2018; Zhang et al., 2007; Zhao et al., 2018a), which has the character of highly selective recognition capacity and good sensitivity (Zhang and Seelig, 2011). The strand displacement is initiated by the hybridization between target gene and a short single-stranded domain called "toehold" (typically consists of 5–8 nucleotides (nt)), leading to displacing another strand from the substrate (Gao et al., 2014; Zhang et al., 2010). This technique has been used frequently to detect nucleic acid (Li et al., 2019a; Wang et al., 2017a; Yin et al., 2017; Zhang et al., 2018a,b). The traditional TMSD-based methods usually allow a specified input oligonucleotide (target) to initiate a corresponding specified output and another waste strand. Then fuel strand can help target DNA to activate the next cycle of the strand displacement reaction. This traditional single output limits the signal amplification efficiency. To further increase the efficiency and improve the sensitivity, we developed a kind of elaborate design strategy through the converting of one input to two strands output within one strand displacement cycle (called it "dual-output TMSD") to realize the efficient signal amplification for DNA detection.

In this work, a novel homogeneous electrochemical biosensor based on dual-output TMSD to detect specie-specific DNA sequences for animal species determination was constructed. Bovine-specific DNA sequence is selected as a model target, because beef is at high risk of adulteration worldwide. The target recognition, strand displacement amplification, as well as the enzymatic reaction was performed in the solution phase instead of on the electrode surface, avoiding the tedious modification procedure and low hybridization efficiency. The proposed elaborate design dual-output TMSD platform exhibited high signal amplification efficiency and good selectivity. Furthermore, the established biosensor was eventually employed to identify the specie-specific genomic DNA sequences from 13 different species (including cattle, sheep, pig, horse, etc.) with a satisfactory result.

2. Experimental section

2.1. Reagents

All oligonucleotides used in this work with high-performance liquid chromatography (HPLC) purification were synthesized by Sangon Inc. (Shanghai, China), and the sequences are shown below:

Target DNA (T, Bovine): 5′-CCT TCA GAG AGG GTC CCA CTG GTC C-3'.

Linker (L): 5′-*GGA CCA GTG GGA CCC TCT CTG AAG GTA GGG* GGG ACC CTC TCT GAA GGT AGG G-3' (the letters in italic represent the complementary domains of target DNA, the letters with underline, and wave line are toehold 1 and toehold 2, respectively).

Methylene blue labeled probe (MB-P): 5′-MB-CCC TAC CTT CAG AGA GGG TCC C-3'.

Probe (P): 5′-CCC TAC CTT CAG AGA GGG TCC C-3' (label-free but with the same sequence as MB-P).

Fuel (F): 5′-AGA GGG TCC CCC CTA CCT TCA GAG AGG GTC CC-3'.

Single-base mismatched DNA (SM): 5′-CCT TCA GAG AGG TTC CCA CTG GTC C-3' (underlined letter denotes the mismatched base).

Two-base mismatched DNA (TM): 5′-CCT TCA GAG AGC TTC CCA CTG GTC C-3' (underlined letters denote the mismatched bases).

Noncomplementary DNA (NC): 5′-TGA GCG CAT CAT GGG CCA GAC ACT TT-3'.

Exonuclease I (Exo I), and its corresponding buffer were obtained from Thermo (Shanghai, China). Nafion® perfluorinated resin solution was purchased from Sigma-Aldrich (Shanghai, China). All chemicals were of analytical reagent grade and used directly without further purification. Ultrapure water (Milli-Q, Millipore, resistance 18.2 MΩ·cm) was used in the whole experiments.

2.2. ITO electrode pretreatment and instrument

The differential pulse voltammetry (DPV) signal measurements were performed on a CHI660D electrochemical workstation (Chenhua Instruments, Shanghai, China). All electrochemical measurements were conducted on a three-electrode system including an ITO working electrode (the working area was 5 mm × 3 mm), an Ag/AgCl reference electrode and a platinum wire counter electrode. The DPV signals were recorded with the potential ranging from 0.1 to −0.6 V in Buffer 1 (10 mM Tris HCl, 50 mM NaCl, 10 mM $MgCl_2$, 1 mM DTT, pH 7.9). The negative charged ITO working electrode surface was accomplished after the following treatments: Initially, the ITO electrode was sonicated in an alconox solution (1 g of alconox/100 mL of double-distilled water) for 15 min, isopropanol for 15 min, and twice in double-distilled water for 10 min in turn (Xuan et al., 2013). Subsequently, the cleaned ITO electrode was immersed into Nafion® perfluorinated resin solution for 5 s and dried naturally to form a polymer film on the electrode surface with stable negative charge.

2.3. Dual-output TMSD-based bovine-specific DNA sequence detection

All oligonucleotides were initially dissolved in Buffer 1, respectively, to obtain the stock solutions with final concentration of 10 μM (stored at 4 °C). Prior to TMSD, 2.5 μM L and 5.0 μM MB-P were denatured at 95 °C for 5 min and cooled down to 25 °C at a slow rate to form the DNA duplex (called Substrate, S). As for the DNA assay, a volume of 40 μL Buffer 1 containing 10 μL of S, 500 nM F and 20 U Exo I were mixed with different concentrations of target DNA, simultaneously, and then incubated at 37 °C for 2 h. The control experiment was performed under the same condition in the absence of target DNA. Then, the DPV signals of the mixture on the Nafion modified electrodes were recorded, and all measurements were carried out at room temperature (25 ± 1.0 °C) and repeated three times.

2.4. Gel electrophoresis

Polyacrylamide gel electrophoresis (PAGE, 12%) was employed to verify the establishment of the proposed biosensor. MB-P in native PAGE was replaced by label-free probe (P) having the same sequence, such that the fluorescence intensity of the hybrid product was not affected in the gel. The project was run in 0.5 × TBE buffer (Tris/Boric acid, pH 8.2) at a constant voltage of 80 V for 90 min at room temperature.

2.5. Detection of specie-specific DNA sequences in real samples

The skeletal muscles from 13 species including cattle (*Bos Taurus*), sheep (*Ovis aries*), pig (*Sus scrofa*), horse (*Equus caballus*), donkey (*Equus asinus*), dog (*Canis lupus familiaris*), fox (*Vulpes vulpes*), rabbit (*Oryctolagus cuniculus*), mouse (*Mus musculus*), rat (*Rattus norvegicus*), chicken (*Gallus gallus*), duck (*Anas platyrhynchos*) and goose (*Anser cygnoides domesticus*) were employed as experimental materials. Sample source has been summarized in Table S1 in the supplemental information (SI). Two grams of muscle were used to extract genomic DNA according to the proteinase K-SDS-phenol/chloroform protocol (Orkin, 1990). Then, the extracted genomic DNA (40 ng/μL) of each species was kept on ice and sheared to 100–200 bp short DNA fragments using a 130-Watt ultrasonic processor (Sonics & Materials, CT, USA) at 60% duty for 20 cycles of 40 s ON and 20 s OFF according to the manufacturers' instruction. Subsequently, the measurement procedure for the extracted DNA fragments detection was the same as that using the target DNA standard solution (see 2.3).

3. Results and discussion

3.1. Principle of the homogeneous electrochemical biosensor for bovine-specific DNA sequence detection

The detailed mechanism of the dual-output TMSD based homogeneous electrochemical biosensor for the sensitive detection of bovine-specific DNA sequence was illustrated in Scheme 1. Initially, a double-stranded DNA (S) with toehold 1 consisting of 8 nt was initially formed by the hybridization between carefully designed one L and two

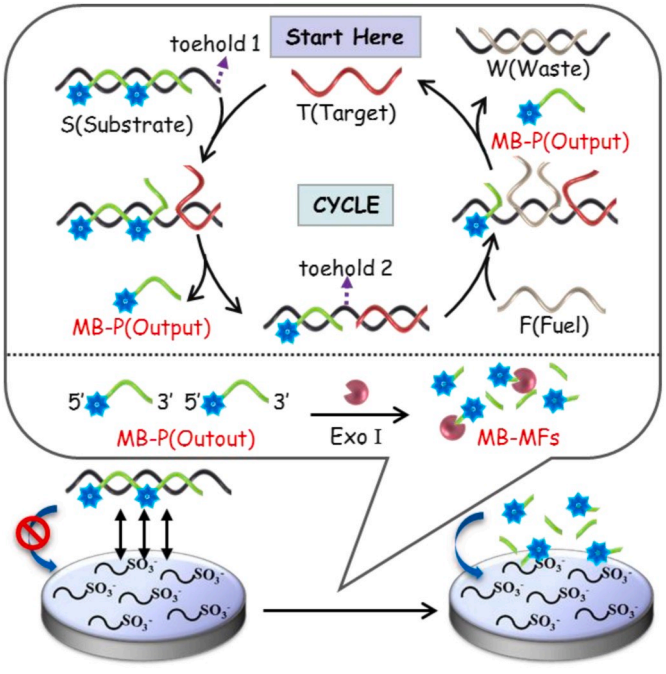

Scheme 1. Schematic illustration of the homogeneous electrochemical biosensor for bovine-specific DNA sequence detection.

MB-P with duplex structure, so the MB-P in S could not be digested by Exo I (acting on single-stranded DNA in a 3′ to 5′ direction, releasing deoxyribonucleoside 5′-monophosphates in a stepwise manner). The DNA duplex could diffuse hardly to the electrode surface owing to the strong electrostatic repulsion between S and the negatively charged ITO electrode. Therefore, the electrochemical signal molecule MB was far from the electrode surface, resulting in low DPV signal detected. The present of target DNA could hybrid with the toehold 1 and caused the displaced of MB-P (as output strand) from the S, accompanied by the exposure of toehold 2. Subsequently, F was introduced to bind with the toehold 2 and could initiate a second branch migration reaction, resulting in the release of second MB-P and target DNA. The released target DNA could bind to S again, initiating a cyclic reaction. Therefore, one target DNA could cause the production of large amount of MB-P. Since MB-P still contained relative large amount of negative charges, its diffusion to the ITO surface was still relative low. Then Exo I was introduced into the system, which could degrade plenty of released MB-P in stepwise in a 3′ to 5′ direction, and cause the producing of large amount of short MB-labeled mononucleotides fragments (MB-MFs) in the sensing system. The MB-MFs contained less negative charges and could easily diffuse towards negatively charged ITO electrode surface, so a dramatically enhanced electrochemical signal was detected. The DPV signal detected had some relationship with the target DNA concentration. So, a homogeneous electrochemical strategy for target DNA detection based on dual-output TMSD could be realized.

3.2. Characterization of the modified ITO electrode

Initially, the scanning electron microscope (SEM) and energy dispersive spectroscopy (EDS) were conducted to study the interface of the electrode. As shown in Fig. 1A, the right light grey was bare ITO electrode, and the left dark grey shading indicated Nafion modified ITO electrode. The prepared Nafion modified ITO electrode had a smooth surface in high-resolution SEM image. And the EDS experiment (Fig. 1B) was employed for the elemental analysis of the surface on ITO electrode. Compared with the bare ITO electrode (right), the F element content on the Nafion modified ITO electrode (left) was obviously higher, and the In element had the similar content. These results indicated that the ITO electrode was successfully modified by Nafion with a smooth surface. In addition, the interface properties of electrode were further characterized by the electrochemical impedance spectroscopy (EIS), shown in Fig. 1C. The inset in Fig. 1C is the equivalent circuit model of the work electrode used to model the EIS data. The equivalent circuit includes four parts, R_s is the electrolyte resistance, C_{dl} denotes double layer capacitance, Z_w represents Warburg impedance and R_{et} represents the charge transfer resistance that affected by the surface modification. The R_{et} can be equal to the semicircle diameter in Fig. 1C, which can intuitively reflect the electron-transfer kinetics of the $[Fe(CN)_6]^{3-/4-}$ at the interface of electrode. When the Nafion was modified on the ITO electrode surface, R_{et} would be increased. The solid lines in Fig. 1C were the theoretical fit of the impedance data with the help of equivalent circuit with good fitting between the simulated and experimental spectra. As shown in Fig. 1C, the bare ITO electrode showed a very small semicircle ($R_{et} \approx$ 150 Ω, curve a), indicating the weak resistance. The R_{et} increased evidently to approximately 4400 Ω after the modification of Nafion on the bare ITO electrode surface (curve b). The reason lies in that the electrostatic repulsion is enhanced between the negatively charged Nafion layer and $[Fe(CN)_6]^{3-/4-}$, and the conductivity of Nafion is not so good. However, the incubation with the MBFs caused the obviously decreased resistance ($R_{et} \approx$ 1200 Ω, curve c). This is because that the MB-MFs are smaller and contain less negative charges, which can diffuse easily to the negatively charged ITO electrode surface. In addition, the MBFs might inset the Nafion film to increase the conductivity, and further help the electron transfer. These above evidence illustrated that the MBFs could be accumulated on the surface of ITO electrode, which was modified by Nafion and had plenty of negative charges.

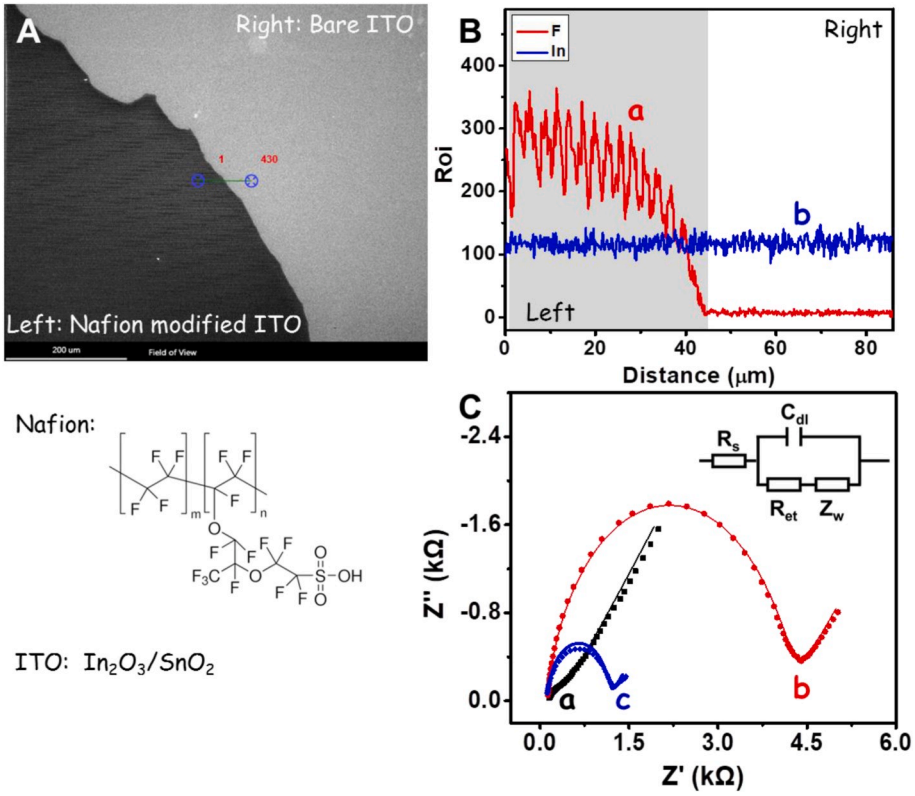

Fig. 1. (A) SEM image and (B) EDS analysis (line scan) of the Nafion modified ITO (left) and bare ITO (right) electrode. (C) Nyquist diagrams of different electrodes in 5 mM $[Fe(CN)_6]^{3-/4-}$ with 100 mM KCl electrolyte: (a) bare ITO electrode, (b) Nafion modified ITO electrode, (c) Nafion modified ITO electrode after incubating with MBFs. Inset: the equivalent circuit of the Nyquist plots. The solid lines show the theoretical fit of the impedance data according to the equivalent circuit. The frequency range was from 0.1 Hz to 10 kHz with amplitude of 5 mV. The quiet time was 2 s. A three-electrode system including a Nafion modified ITO working electrode, an Ag/AgCl reference electrode and a platinum wire counter electrode were used.

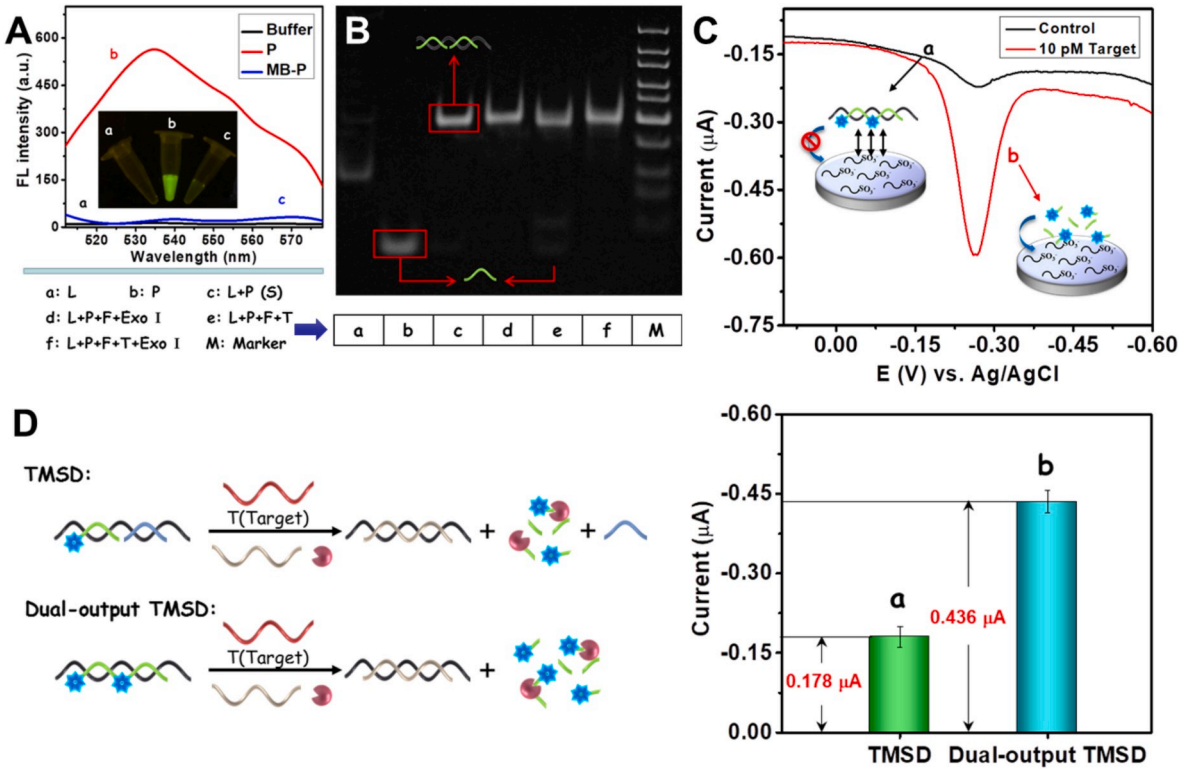

Fig. 2. (A) Fluorescence spectra of different conditions: (a) buffer, (b) P, (c) MB-P, which was mixed with 1 × SYBR Gold, respectively. Inset: the corresponding pictures in the ultraviolet lamp. (B) Polyacrylamide gel electrophoresis (12%) analysis of different conditions: (a) L, (b) P, (c) L + P, (d) L + P + F + Exo I, (e) L + P + F + T (f) L + P + F + T + Exo I, (M) DNA marker. (C) DPV signal of the proposed biosensor in the (a) absence and (b) presence of 10 pM target. (D) Comparison of the DPV signal between the traditional TMSD method and the proposed dual-output TMSD method in the presence of 10 pM target. (For interpretation of the references to color in this figure legend, the reader is referred to the Web version of this article.)

3.3. Feasibility of the proposed sensing platform

PAGE is a reliable electrophoresis technique to verify the length and conformation of DNA. Initially, we used the PAGE experiment under different conditions to characterize the dual-output TMSD process. The MB would affect the PAGE imaging of MB-P, the corresponding data of fluorescence intensity were shown in Fig. 2A. There was no fluorescence intensity in the buffer containing the nucleic acid dye of SYBR Gold (lane a), and the addition of label-free probe (P) would lead to an obvious fluorescence signal (lane b). When the MB-P mixed with SYBR Gold, there was nearly no fluorescence signal (lane c). So the MB-P was replaced by P in the PAGE analysis. As shown in Fig. 2B, the single L (lane a) was migrated more slowly than the P (lane b), due to the nucleotide bases of L were more than P. After the hybridization between L and P, a slower moving band (lane c) was observed, indicating the formation of S. The addition of F and Exo I to S in the absence of target (T), no obvious changes (lane d) was detected, and this revealed the proposed TMSD could not be triggered without target DNA, and S could resist the digestion of Exo I. In order to verify the target-induced TMSD process, the S was firstly treated by F and T, new band in the same position as lane b was generated (lane e), implying the release of P. Briefly, the TMSD was initiated and efficient. With the further addition of Exo I, the generated band in lane e was gone (lane f). Namely, the released P was digested by Exo I. These results clearly verified the successful fabrication of the proposed TMSD strategy.

Furthermore, DPV experiment was performed to verify the feasibility of the designed system (Fig. 2C). In the absence of target DNA, a weak DPV signal was observed (curve a), showing that the MB-P in S could not be digested by Exo I. Hence, the negatively charged MB-P was hardly close to the same negatively charged ITO electrode surface because of electrostatic repulsion. By comparison, a significantly increased electrochemical signal was obtained when the target DNA was introduced (curve b), which was ascribed to the startup of dual-output TMSD amplification and enzyme digestion of Exo I. Multiple MB-P from S were released through the process of dual-output TMSD, which was induced by the target DNA. And the free MB-P could be degraded by Exo I in a 3′ to 5’ direction, releasing less negative charged MB-MFs in stepwise, which could easily disperse to the surface of ITO electrode. Hence, an obviously DPV signal was recorded. These results indicated that the feasibility of the designed sensing platform was verified with the help of PAGE and DPV.

To clarify the high signal amplification efficiency of the developed strategy, the DPV responses between the conventional TMSD and the proposed dual-output TMSD were compared. As shown in Fig. 2D, the target initiated the TMSD amplification reaction and produced electrochemical signal (column a, 0.178 μA). In comparison, a significantly increased current response (column b, 0.436 μA) was recorded when the developed dual-output TMSD was introduced. The reason might be attributed to amounts of MB-P generated by the dual-output TMSD process than the traditional TMSD, indicating that this work exhibited more favorable high efficient amplification.

3.4. Optimization of the experimental conditions

To achieve the best analytical performance, the experimental conditions that could affect the designed biosensor were systematically optimized, containing the concentration of Nafion, fuel strand, Exo I, and the reaction time of Exo I. As shown in Fig. 3, the ΔI was the difference of the peak current in the presence and absence of target DNA.

The concentration of Nafion modified on the ITO electrode, which could affect the quantity of negative charge on the electrode surface, directly influenced the generated DPV signal. Different concentrations of Nafion ranging from 0 to 1% were used for the modification of the ITO electrodes. As shown in Fig. 3A, the maximum ΔI was obtained when the Nafion concentration was 0.5%. Less concentration of Nafion modified ITO electrode could lead to less negative charge on the surface, and low DPV signal was recorded. However, excessive amount of Nafion would cause the too thickness of Nafion layer to hinder the electron transfer on the ITO electrode surface, resulting in the decrease of peak current. Therefore, 0.5% Nafion was chosen as the optimal concentration for the ITO electrodes modification.

Fuel is also one of the key parameter on the dual-output TMSD process. Fig. 3B showed the effect of the fuel concentration on the electrochemical signal. The ΔI first increased when the fuel

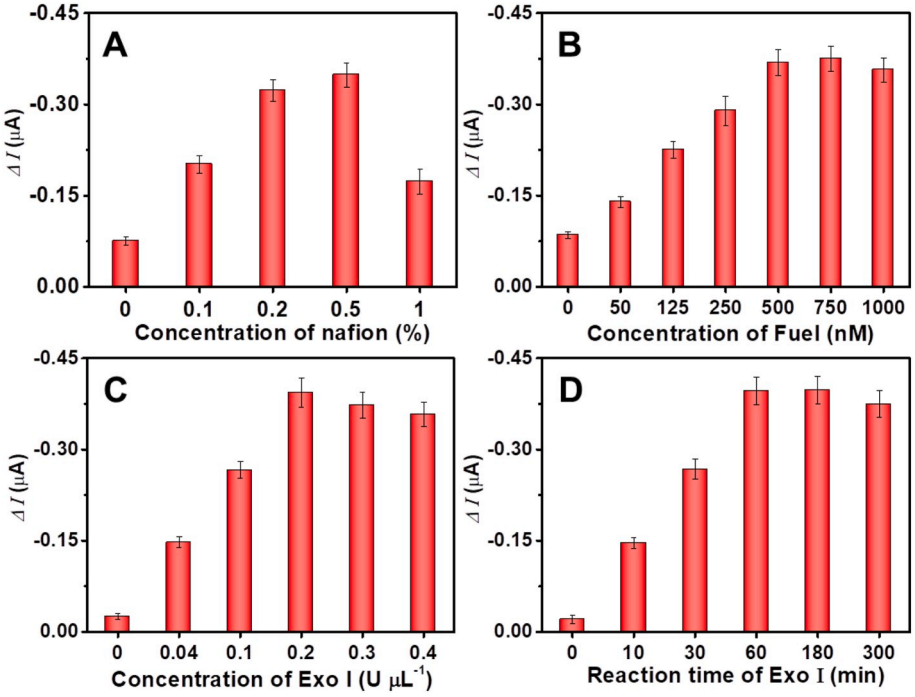

Fig. 3. The effects of different conditions: the concentration of (A) Nafion, (B) Fuel, (C) Exo I, (D) the reaction time of Exo I digestion. (10 pM target used in these cases).

concentration increased, and then reached a plateau after 500 nM. So, 500 nM fuel was selected as the optimal condition for the following study.

Furthermore, the pH value of the system, concentration and digestion time of Exo I directly affect the electrochemical signal in the analysis system. The pH could mainly affect the activities of Exo I. The influence of different pH values from 3 to 10 were explored. The electrochemical signals increased with the increasing of pH value firstly and reached a plateau in the range of pH 6.8–9.0 and then decreased. Considering the optimization results, physiological conditions, an intermediate value 7.9 was chosen in this work. Subsequently, the different concentrations of Exo I were investigated. As shown in Fig. 3C, the ΔI enhanced obviously as the concentration rose up to 0.2 U μL^{-1}, but then the difference of peak current decreased slightly after 0.2 U μL^{-1}. This is mainly because the background signal increased by the nonspecific cleavage at high concentration of Exo I. Hence, the amount of Exo I was set at 0.2 U μL^{-1}. Finally, different reaction time of Exo I ranging from 0 to 300 min was assessed for the digestion of output MB-P in the analysis system (Fig. 3D). The response signal gradually increased with the prolonged reaction time and reached a plateau after 60 min. Therefore, 60 min was selected as the digestion time in this sensing system.

3.5. Analytical performance of the homogeneous electrochemical biosensor

The quantitative range of the proposed homogeneous electrochemical biosensor for bovine-specific DNA sequence detection was evaluated by incubating different concentrations of target under the optimal conditions (Fig. 4). The DPV signal gradually enhanced with the increased concentration of target (Fig. 4A), and the plot of the DPV response exhibited a good linearity with the logarithm of the target concentration in the range from 0.01 pM to 100 pM. The linear-regression equation of the biosensor was ΔI (μA) = −0.1315 lg C_{target} (pM) − 0.2710 with a correlation coefficient of 0.9937 (Fig. 4B). The limit of detection (LOD) was calculated to be 8.2 fM based on the traditional approach reported in the previous references (MacDougall and Crummett, 1980; Nie et al., 2019). The proposed homogeneous electrochemical strategy showed satisfied analytical performance with a lower LOD and wider linear response range compared with other previously reported methods that concentrated on DNA detection (Table 1). (Li et al., 2019b; Su et al., 2015; Tian et al., 2018; Wang et al., 2017b; Zhu et al., 2018) And it also effectively avoided the tedious procedures related with homogeneous immobilization-free electrode. Such exceptional performance was ascribed to the high efficiency of dual-output TMSD amplification and homogeneous approach.

Table 1
Comparison between other strategies and the developed homogeneous electrochemical biosensor for DNA detection.

Method	Dynamic range	Detection limit	Detection time	References
Fluorescence method	25–700 pM	8 pM	20 min	Li et al. (2019b)
Ferromagnetic resonance biosensor	7.8–250 pM	1 pM	80 min	Tian et al. (2018)
Fluorescent biosensor	3.3–33 pM	0.5 pM	325 min	Su et al. (2015)
SERS-based lateral flow assay biosensor	0.1–100 pM (KSHV) 0.2–100 pM (BA)	43 fM (KSHV) 74 fM (BA)	>overnight	Wang et al. (2017b)
Scattering measurement of single particle	0.1 pM to 1 nM	30 fM	45 min	Zhu et al. (2018)
The proposed method	0.01 pM–100 pM	8.2 fM	60 min	This work

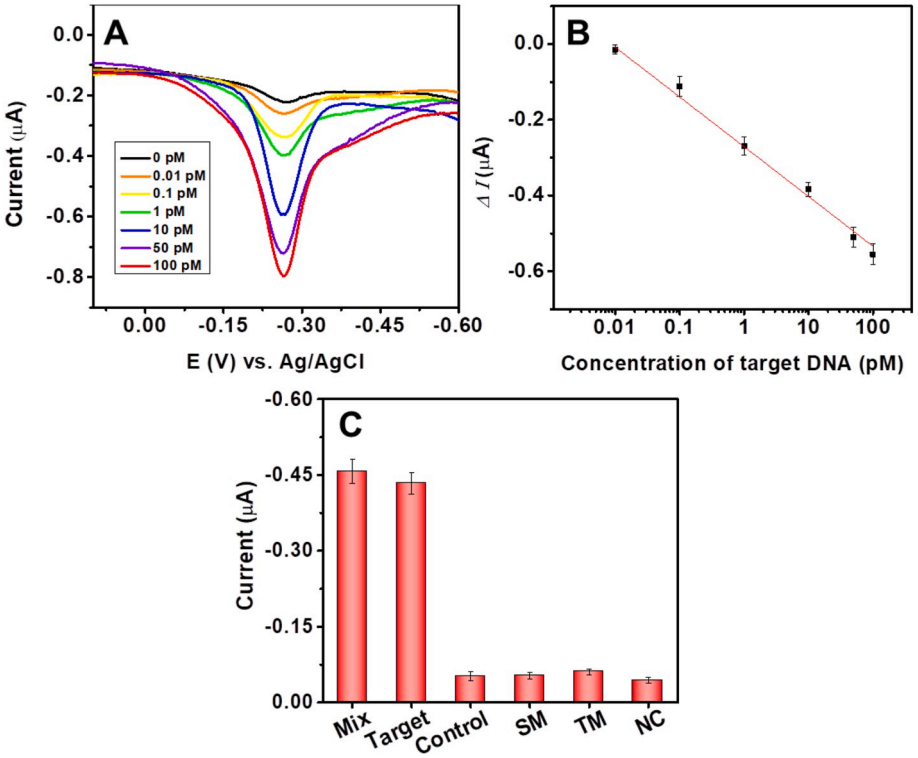

Fig. 4. (A) DPV response at different target bovine-specific DNA sequence concentrations. (a–g) 0, 0.01 pM, 0.1 pM, 1 pM, 10 pM, 50 pM, 100 pM. (B) The calibration curve between ΔI and the logarithm of the target concentration. (C) Selectivity of the proposed dual-output TMSD method. The concentration of interferences was set 100 pM, and the target was 10 pM.

3.6. Selectivity and reproducibility

To investigate the selectivity of the protocol, a series of oligonucleotides including single-base mismatched (SM), two-base mismatched (TM) and noncomplementary (NC) DNA as the interferences, were performed by the homogeneous electrochemical biosensor. As shown in Fig. 4C, the presence of target (10 pM) can cause great current change, but the presence of SM (100 pM) and TM (100 pM) cause very small signal change (a little bigger than the control). The addition of NC (100 pM) cause nearly no signal change. The mixture containing target (10 pM), SM (100 pM), TM (100 pM), and NC (100 pM) exhibited a similar strong current intensity. The detected concentration of target was 9.13 pM with the relative standard deviations (RSD) of 4.93%, and the measured concentration of mixture was 11.98 pM with RSD of 5.12%. This difference is presumed mainly due to interference on electrochemical signal caused by the high concentrations of SM and TM. But it can be identified easily during the species identification since different sequence of DNAs cause greatly change of the response.

Additionally, we further studied the reproducibility of the proposed biosensor by the RSD in a within-batch (intra-assay) and in various batches (inter-assay). The working electrode was repeatedly detected ten times, having an intra-assay RSD of 5.31% And the RSD of inter-assay on ten electrodes was 5.95%. These results confirmed that the proposed homogeneous electrochemical assay had a good analytical reproducibility.

3.7. Real sample analysis for animal species identification

Short DNA fragments, extracted by 13 species meat containing cattle (target), sheep, pig, horse, donkey, dog, fox, rabbit, mouse, rat, chicken, duck and goose, were tested respectively by the developed method to further evaluate the analytical capacity in animal species identification. There are at least four bases differences between bovine-specific DNA sequence (NC_037350.1:10955785–10955809) and homologous DNA sequences of the other 12 species (specificity and conservation analysis of bovine-specific DNA sequence was shown in Fig. 1). As shown in Fig. 5 (original data was shown in Fig. S2), an obvious increase in DPV signal was obtained when the cattle sample was existed, while the currents generated by other species showed no significant differences from the control experiment. Additionally, the measured concentration of specific DNA sequence from cattle (target) by the developed electrochemical sensor was 0.355 ± 0.069 pM. While the detected concentrations of homologous DNA sequences from other species were about 0.01 pM (mouse and goose were lower than the detection limits of the proposed method), obviously lower than that of target group (the determination results for these real samples were shown in Table S2). The RSD of real samples was around 15%–20%, which was mainly because the extracted genomic DNA from actual samples contain a large number of non-specific DNA sequences. According to the guidance on validation and verification of chemical analytical methods (GB/T 27417–2017, Figure B1), the RSD of real sample measurements was acceptable. In summary, these results demonstrated the approving accuracy of our approach, and promising potential application for animal species identification.

4. Conclusion

In conclusion, an efficient and specific assay of bovine-specific DNA sequence combining the advantage of homogeneous electrochemical approach and dual-output TMSD amplification was demonstrated. The target recognition, dual-output TMSD amplification, and the enzymatic digestion reaction were implemented in the homogeneous solution, simplifying the operational procedures and improving the hybridization efficiency compared with the reaction occurred in electrode surface. Additionally, the designed dual-output TMSD amplification exhibited satisfactory sensing performance with high sensitivity (a LOD of 8.2 fM could be obtained) and good selectivity (having discrimination ability of single-base mismatch DNA). The specie-specific DNA sequences, extracted by many species meat, were evaluated by the proposed biosensor and achieved an ideal result. Therefore, this work had great potential for the animal species identification and meat adulteration.

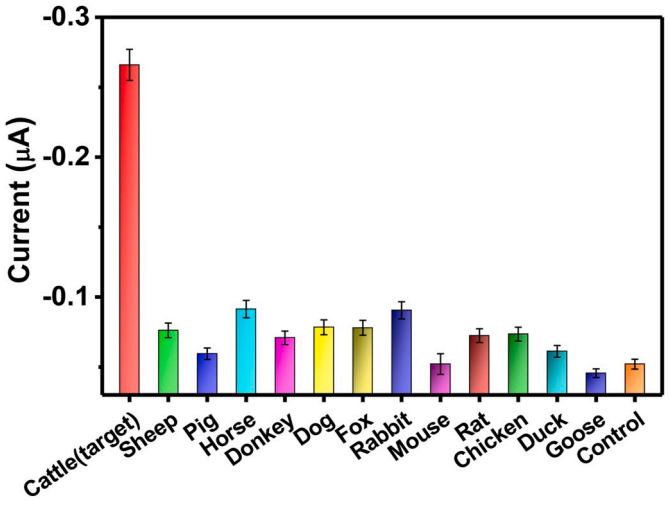

Fig. 5. Application of the prepared homogeneous electrochemical biosensor in animal species identification.

Declaration of competing interest

The authors declare that they have no known competing financial interests or personal relationships that could have appeared to influence the work reported in this paper.

CRediT authorship contribution statement

Ying Zhang: Conceptualization, Investigation, Writing - original draft. **Wenjun Wang:** Conceptualization, Investigation, Data curation. **Zhenyu Lin:** Writing - review & editing, Supervision. **Bang Liu:** Funding acquisition, Supervision. **Xiang Zhou:** Writing - review & editing, Funding acquisition, Supervision.

Acknowledgements

This project was financially supported by National Science and Technology Major Project of China (2018ZX08012-001-010) and Fundamental Research Funds for the Central Universities (2662018QD004).

Appendix A. Supplementary data

Supplementary data to this article can be found online at https://doi.org/10.1016/j.bios.2020.112256.

References

Ali, M.E., Ahamad, M.N.U., Asing, Hossain, M.A.M., Sultana, S., 2018. Food Contr. 84, 148–158.
Bilge, G., Velioglu, H.M., Sezer, B., Eseller, K.E., Boyaci, I.H., 2016. Meat Sci. 119, 118–122.
Cai, Q.F., Wang, X.C., Liu, G.M., Zhang, L., Ruan, M.M., Liu, Y., Cao, M.J., 2013. Food Contr. 29 (1), 241–247.
Chang, J., Li, H., Li, F., 2019a. Chem. Commun. 55 (71), 10603–10606.
Chang, J., Wang, X., Wang, J., Li, H., Li, F., 2019b. Anal. Chem. 91 (5), 3604–3610.
Chen, X., Huang, J., Zhang, S., Mo, F., Su, S., Li, Y., Fang, L., Deng, J., Huang, H., Luo, Z., Zheng, J., 2019. ACS Appl. Mater. Interfaces 11 (4), 3745–3752.
Doosti, A., Dehkordi, P.G., Rahimi, E., 2014. J. Food Sci. Technol. 51 (1), 148–152.
Druml, B., Hochegger, R., Cichna-Markl, M., 2015. Food Contr. 57, 370–376.

Gao, Z.F., Ling, Y., Lu, L., Chen, N.Y., Luo, H.Q., Li, N.B., 2014. Anal. Chem. 86 (5), 2543–2548.
Henihan, G., Schulze, H., Corrigan, D.K., Giraud, G., Terry, J.G., Hardie, A., Campbell, C. J., Walton, A.J., Crain, J., Pethig, R., Templeton, K.E., Mount, A.R., Bachmann, T.T., 2016. Biosens. Bioelectron. 81, 487–494.
Hong, F., Chen, X.X., Cao, Y.T., Dong, Y.R., Wu, D.Z., 2018. Biosens. Bioelectron. 112, 202–208.
Hsieh, Y.-H.P., Ofori, J.A., 2014. J. Agric. Food Chem. 62 (52), 12536–12544.
King, T., Cole, M., Farber, J.M., Eisenbrand, G., Zabaras, D., Fox, E.M., Hill, J.P., 2017. Trends Food Sci. Technol. 68, 160–175.
Koo, B., Yorita, A.M., Schmidt, J.J., Monbouquette, H.G., 2018. Lab Chip 18 (15), 2291–2299.
Leitner, A., Castro-Rubio, F., Marina, M.L., Lindner, W., 2006. J. Proteome Res. 5 (9), 2424–2430.
Li, H., Zhang, Y., Luo, Y., Sun, X., 2011a. Small 7 (11), 1562–1568.
Li, H.L., Luo, Y.L., Sun, X.P., 2011b. Biosens. Bioelectron. 27 (1), 167–171.
Li, Q., Liu, Z., Zhou, D., Pan, J., Liu, C., Chen, J., 2019a. Analyst 144 (6), 2173–2178.
Li, Y., Liu, W., Zhu, Y., Diao, L., 2019b. J. Med. Virol. 91 (6), 979–985.
Lin, W.-F., Hwang, D.-F., 2007. Food Contr. 18 (9), 1050–1057.
Lin, C., Zheng, H., Huang, Y., Chen, Z., Luo, F., Wang, J., Guo, L., Qiu, B., Lin, Z., Yang, H., 2018. Biosens. Bioelectron. 117, 474–479.
Lu, L., Su, H., Li, F., 2017. Anal. Chem. 89 (16), 8328–8334.
Luo, X., Lee, T.M.-H., Hsing, I.M., 2008. Anal. Chem. 80 (19), 7341–7346.
MacDougall, D., Crummett, W.B., 1980. Anal. Chem. 52 (14), 2242–2249.
Nie, Y.M., Yuan, X.D., Zhang, P., Chai, Y.Q., Yuan, R., 2019. Anal. Chem. 91 (5), 3452–3458.
O'Mahony, P.J., 2013. Q. J. Med. 106 (6), 595–597.
Orkin, S., 1990. Nature 343 (6259), 604–605.
Piskata, Z., Pospisilova, E., Borilova, G., 2017. Int. J. Food Prop. 20, S430–S443.
Piskata, Z., Servusova, E., Babak, V., Nesvadbova, M., Borilova, G., 2019. Mol 24 (6), 1188.
Sapkota, K., Kaur, A., Megalathan, A., Donkoh-Moore, C., Dhakal, S., 2019. Sensors 19 (16), 3495.
Shi, Z., Yin, B., Li, Y., Zhou, G., Li, C., Xu, X., Luo, X., Zhang, X., Qi, J., Voglmeir, J., Liu, L., 2019. J. Agric. Food Chem. 67 (37), 10543–10551.
Su, C., Liu, Y., Ye, T., Xiang, X., Ji, X., He, Z., 2015. Anal. Chim. Acta 853, 495–500.
Tan, Y., Wei, X.F., Zhao, M.M., Qiu, B., Guo, L.H., Lin, Z.Y., Yang, H.-H., 2015. Anal. Chem. 87 (18), 9204–9208.
Tian, B., Liao, X., Svedlindh, P., Stromberg, M., Wetterskog, E., 2018. ACS Sens. 3 (6), 1093–1101.
Wang, L., Zhang, Y.W., Tian, J.Q., Li, H.L., Sun, X.P., 2011. Nucleic Acids Res. 39 (6), e37.
Wang, S., Yang, F., Jin, D., Dai, Q., Tu, J., Liu, Y., Ning, Y., Zhang, G.-J., 2017a. Anal. Chem. 89, 5349–5356.
Wang, X., Choi, N., Cheng, Z., Ko, J., Chen, L., Choo, J., 2017b. Anal. Chem. 89 (2), 1163–1169.
Wang, W., Liu, J., Zhang, Q., Zhou, X., Liu, B., 2019. Food Contr. 105, 29–37.
Wei, X., Ma, X., Sun, J.-j., Lin, Z., Guo, L., Qiu, B., Chen, G., 2014. Anal. Chem. 86 (7), 3563–3567.
Xuan, F., Luo, X., Hsing, I.M., 2013. Anal. Chem. 85 (9), 4586–4593.
Yang, L., Liu, D., Hao, S., Qu, F., Sun, X., 2017. Anal. Chem. 89 (4), 2191–2195.
Yin, D., Tao, Y., Tang, L., Li, W., Zhang, Z., Li, J., Xie, G., 2017. Microchim. Acta 184 (10), 3721–3728.
Zhang, D.Y., Seelig, G., 2011. Nat. Chem. 3 (2), 103–113.
Zhang, D.Y., Turberfield, A.J., Yurke, B., Winfree, E., 2007. Science 318 (5853), 1121–1125.
Zhang, Z., Zeng, D.D., Ma, H.W., Feng, G.Y., Hu, J., He, L., Li, C., Fan, C.H., 2010. Small 6 (17), 1854–1858.
Zhang, N., Shi, X.-M., Guo, H.-Q., Zhao, X.-Z., Zhao, W.-W., Xu, J.-J., Chen, H.-Y., 2018a. Anal. Chem. 90 (20), 11892–11898.
Zhao, J., Zheng, T., Gao, J., Xu, W., 2018b. Electrochim. Acta 274, 16–22.
Zhu, L., Li, G., He, Y., Tan, H., Sun, S., 2018. Talanta 178, 545–551.